

Improving the purity of heralded single-photon sources through spontaneous parametric down-conversion process

Jing Wang(王静), Chun-Hui Zhang(张春辉), Jing-Yang Liu(刘靖阳), Xue-Rui Qian(钱雪瑞), Jian Li(李剑), and Qin Wang(王琴)

Citation: Chin. Phys. B, 2021, 30 (**7**): 070304. DOI: 10.1088/1674-1056/abfb5c
Journal homepage: http://cpb.iphy.ac.cn; http://iopscience.iop.org/cpb

What follows is a list of articles you may be interested in

Quantum computation and error correction based on continuous variable cluster states

Shuhong Hao(郝树宏), Xiaowei Deng(邓晓玮), Yang Liu(刘阳), Xiaolong Su(苏晓龙), Changde Xie(谢常德), and Kunchi Peng(彭堃墀)

Chin. Phys. B, 2021, 30 (**6**): 060312. DOI: 10.1088/1674-1056/abeb0a

Quantum computation and simulation with vibrational modes of trapped ions

Wentao Chen(陈文涛), Jaren Gan, Jing-Ning Zhang(张静宁), Dzmitry Matuskevich, and Kihwan Kim(金奇奂)

Chin. Phys. B, 2021, 30 (**6**): 060311. DOI: 10.1088/1674-1056/ac01e3

Dynamics of bright soliton in a spin-orbit coupled spin-1 Bose-Einstein condensate

Hui Guo(郭慧), Xu Qiu(邱旭), Yan Ma(马燕), Hai-Feng Jiang(姜海峰), and Xiao-Fei Zhang(张晓斐)

Chin. Phys. B, 2021, 30 (**6**): 060310. DOI: 10.1088/1674-1056/abf34a

Practical decoy-state BB84 quantum key distribution with quantum memory

Xian-Ke Li(李咸柯), Xiao-Qian Song(宋小谦), Qi-Wei Guo(郭其伟), Xing-Yu Zhou(周星宇), and Qin Wang(王琴)

Chin. Phys. B, 2021, 30 (**6**): 060305. DOI: 10.1088/1674-1056/abda31

Wave-particle duality relation with a quantum *N*-path beamsplitter

Dong-Yang Wang(王冬阳), Jun-Jie Wu(吴俊杰), Yi-Zhi Wang(王易之), Yong Liu(刘雍), An-Qi Huang(黄安琪), Chun-Lin Yu(于春霖), and Xue-Jun Yang(杨学军)

Chin. Phys. B, 2021, 30 (**5**): 050302. DOI: 10.1088/1674-1056/abeb0f

---

RAPID COMMUNICATION

Improving the purity of heralded single-photon sources through spontaneous parametric down-conversion process*

Jing Wang(王静)[1,2], Chun-Hui Zhang(张春辉)[1,2], Jing-Yang Liu(刘靖阳)[1,2], Xue-Rui Qian(钱雪瑞)[1,2], Jian Li(李剑)[1,2], and Qin Wang(王琴)[1,2,†]

[1] *Institute of Quantum Information and Technology, Nanjing University of Posts and Telecommunications, Nanjing* 210003, *China*
[2] *Broadband Wireless Communication and Sensor Network Technology, Key Laboratory of Ministry of Education, Nanjing University of Posts and Telecommunications, Nanjing* 210003, *China*

(Received 14 January 2021; revised manuscript received 4 April 2021; accepted manuscript online 26 April 2021)

The high-purity single-photon source plays an important role in the field of quantum information. Usually, it is generated through spontaneous parametric down-conversion process. In this paper, we investigate and summarize a few approaches on obtaining single-photon sources with a high purity using either PPKTP or PPLN nonlinear crystals. Moreover, we present improved schemes to increase the purity based on existing work, corresponding applicable conditions and procedures are discussed and analyzed. Besides, we carry out numerical simulations and show that nearly perfect purity can be reached even without using any filters. Therefore, this work might provide valuable references for the generation and application of high purity single-photon sources.

Keywords: quantum information, quantum communication, nonlinear optics

PACS: 03.67.–a, 03.67.Hk, 42.65.–k **DOI:** 10.1088/1674-1056/abfb5c

1. Introduction

Spectrally factorable photon pair has attracted a lot of attention from scientists since it can furnish a high-purity heralded single-photon source, which is essential for the application of quantum information processing, e.g., quantum cryptography,[1,2] quantum teleportation,[3] and quantum dense coding.[4] Both spontaneous parametric down-conversion (SPDC) and spontaneous four-wave-mixing (SFWM) can generate photon pairs, and the former is more widely utilized compared with the latter due to its simplicity and convenience in experimental preparations. In a SPDC process, when a laser incidents onto a piece of nonlinear crystal, it spontaneously generates photon pairs, one is denoted as the signal photon and the other is named the idle photon. It obeys both the laws of energy conservation and momentum conservation during the SPDC process. In most cases, the signal and the idler photons are spectrally correlated, then one might gather information of one photon after carrying out monitoring on the other one, resulting in side-channel information leakage in some applications, e.g., the quantum key distribution, the quantum random number generator. Therefore, it is very important to obtain spectrally or frequently uncorrelated photon pairs. Usually, purity is used to characterize the correlation degree of a photon pair, and the higher the purity, the lower the correlation in frequency.

To date, different methods for improving the spectral purity of photon pairs have been put forward. For example, Mosley *et al.* and Meyer-Scott *et al.*[5,6] proposed to improve the spectral purity by using narrow bandpass filters, since narrow bandpass filters can effectively filter out unwanted frequencies, and thus destroy the spectral correlations in SPDC sources.[7,8] However, narrow bandpass filters will inevitably bring into extra insertion loss, causing a lower photon counting rate in practical experiments.[6] Moreover, it is difficult to make the spectral shape of each filter identically matched with the photons passing by, since they might come from different crystals.[9] In contrast, another good choice is to select proper nonlinear crystal, pumping laser, and phase-match conditions for improving the spectral purity.

There have been a lot of works addressing this aspect, and in general they can be divided into four categories: (i) to apply Gaussian approximation on the phase matching amplitude and then decompose the joint spectral amplitude (JSA) by selecting proper pump bandwidths and crystal lengths for spectral uncorrelation;[10–13] (ii) to achieve frequency uncorrelated biphotons with group velocity matching (GVM) condition;[13–20] (iii) to process optimizations by adjusting the ratio between the width of the pump envelope amplitude and the width of the phase-matching amplitude;[21] (iv) to implement joint optimizations on both the pump bandwidth and the crystal length.[22] In this paper, we systematically study and

*Project supported by the National Key Research and Development Program of China (Grant Nos. 2018YFA0306400 and 2017YFA0304100), the National Natural Science Foundation of China (Grant Nos. 12074194, 11774180, and U19A2075), and the Leading-edge Technology Program of Jiangsu Natural Science Foundation, China (Grant No. BK20192001).

†Corresponding author. E-mail: qinw@njupt.edu.cn

© 2021 Chinese Physical Society and IOP Publishing Ltd

summarize these existing methods, and further present improved techniques. By re-defining the formula of the ratio between the widths of the phase matching amplitude and the pump envelope amplitude, we can obtain an improved purity with the third method compared with former work. Moreover, by implementing the local search algorithm into the joint optimization process for the fourth approach, we can greatly reduce the time cost on searching the optimal values. We first describe the theory, then carry out corresponding numerical simulations, and finally discuss advantages and disadvantages of each method. To be noted, in principle, the introduced methods can be implemented on any kind of periodically poled nonlinear crystals. Here for simplicity, we just employ the periodically-poled potassium titanylphosphate (PPKTP) crystal and the periodically-poled lithium niobate (PPLN) crystal as examples for illustration.

2. Theory

For a collinear SPDC process, the signal photon and the idle photon are created by driving pump photon into a nonlinear crystal. At the output of the crystal, the biphoton state can be written as

$$|\varphi\rangle = \int_0^\infty \int_0^\infty \mathrm{d}\omega_\mathrm{s}\,\mathrm{d}\omega_\mathrm{i} f(\omega_\mathrm{s},\omega_\mathrm{i})\hat{a}_\mathrm{s}^\dagger(\omega_\mathrm{s})\hat{a}_\mathrm{i}^\dagger(\omega_\mathrm{i})|0\rangle|0\rangle, \quad (1)$$

where ω_s and ω_i are the angular frequencies of the signal and idle photons, respectively; $\hat{a}_\mathrm{s}^\dagger$ and $\hat{a}_\mathrm{i}^\dagger$ are the creation operators of signal and idler, respectively. The function $f(\omega_\mathrm{s},\omega_\mathrm{i})$ is the joint spectral amplitude (JSA), which is obtained by multiplying the pump envelope amplitude (PEA) $\alpha(\omega_\mathrm{s},\omega_\mathrm{i})$ and the phase matching amplitude (PMA) $\phi(\omega_\mathrm{s},\omega_\mathrm{i})$, namely,

$$f(\omega_\mathrm{s},\omega_\mathrm{i}) = \alpha(\omega_\mathrm{s},\omega_\mathrm{i}) \times \phi(\omega_\mathrm{s},\omega_\mathrm{i}). \quad (2)$$

By Schmidt decomposition,[23,24] JSA can be decomposed into the product of two orthogonal basis sets, $\mu_n(\omega_\mathrm{s})$ and $\upsilon_n(\omega_\mathrm{i})$, as

$$f(\omega_\mathrm{s},\omega_\mathrm{i}) = \sum_n c_n \mu_n(\omega_\mathrm{s})\upsilon_n(\omega_\mathrm{i}), \quad \sum_n {c_n}^2 = 1. \quad (3)$$

As a result, the spectral purity p of the biphoton state can be calculated by

$$p = \sum_n c_n^4, \quad (4)$$

which equals to the inverse of the Schmidt number K ($K = 1/\sum_n c_n^4$). Iff the value of one c_i is nonzero, and the left c_n are all zero, we denote it as the pure state. It is easy to see that for a pure state, its purity is equal to 1 and its JSA can be reformulated as $f(\omega_\mathrm{s},\omega_\mathrm{i}) = \mu_\mathrm{t}(\omega_\mathrm{s})\upsilon_\mathrm{t}(\omega_\mathrm{i})$, which means that the signal photon and idle photon are uncorrelated in the joint spectral function.

The PEA can be described by a Gaussian function as

$$\alpha(\omega_\mathrm{s},\omega_\mathrm{i}) = \mathrm{e}^{-\frac{(\omega_\mathrm{s}+\omega_\mathrm{i}-\omega_\mathrm{p0})^2}{2\sigma_\mathrm{p}^2}}, \quad (5)$$

where ω_p0 and σ_p are the central frequency and the bandwidth in frequency of the pump photon. σ_p can be converted into the bandwidth in wavelength $\Delta\lambda$ by

$$\sigma_\mathrm{p} = \frac{2\pi c\Delta\lambda}{{\lambda_\mathrm{p}}^2 - (\frac{\Delta\lambda}{2})^2}, \quad (6)$$

where λ_p is the wavelength of the pump. Due to the energy conservation

$$\omega_\mathrm{p0} = \omega_\mathrm{s0} + \omega_\mathrm{i0}, \quad (7)$$

where ω_s0 and ω_i0 are the central frequencies of the signal photon and idle photon, and we can obtain

$$\alpha(\nu_\mathrm{s},\nu_\mathrm{i}) = \mathrm{e}^{-\frac{(\nu_\mathrm{s}+\nu_\mathrm{i})^2}{2\sigma_\mathrm{p}^2}}, \quad (8)$$

where ν_s and ν_i are the frequency differences between their respective frequencies and central frequencies, i.e., $\nu_\mathrm{s} = \omega_\mathrm{s} - \omega_\mathrm{s0}$ and $\nu_\mathrm{i} = \omega_\mathrm{i} - \omega_\mathrm{i0}$.

The PMA in a nonlinear crystal can be written as

$$\phi(\omega_\mathrm{s},\omega_\mathrm{i}) = \mathrm{sinc}\left(\frac{\Delta kL}{2}\right), \quad (9)$$

where L is the crystal length, and Δk is the difference between the wave-vectors. The wave-vector is given by

$$k = \frac{2\pi n}{\lambda}, \quad (10)$$

where n is the refractive index. And the difference between the wave-vectors in s periodically poled crystal can be written as

$$\Delta k = k_\mathrm{p} - k_\mathrm{s} - k_\mathrm{i} - \frac{2\pi}{\Lambda}, \quad (11)$$

where Λ is the poling period of the periodically poled crystal.

2.1. Uncorrelation obtained from JSA

Ignoring quadratic and higher-order terms, we can expand the wave-vectors around the central frequencies up to the first order in detuning ν_j, i.e., $k_j = k_{j0} + k_j'\nu_j$, where k_j' is the derivative of the wave-vector with respect to the central frequency ω_{j0}, and it is also reciprocal of the group velocity, i.e., $k_j' = \mathrm{d}k_j/\mathrm{d}\omega_j|_{\omega_{j0}} = V_{\mathrm{g},j}^{-1}$. According to the quasi-phase-matching condition

$$\Delta k_0 = k_\mathrm{p0} - k_\mathrm{s0} - k_\mathrm{i0} - \frac{2\pi}{\Lambda} = 0, \quad (12)$$

from Eqs. (10) and (11), we can obtain

$$\Delta k(\nu_\mathrm{s},\nu_\mathrm{i}) = -k_\mathrm{s}'\nu_\mathrm{s} - k_\mathrm{i}'\nu_\mathrm{i} + k_\mathrm{p}'(\nu_\mathrm{s}+\nu_\mathrm{i}). \quad (13)$$

To reach spectral uncorrelation, the spectral distribution of PEA and PMA should be concentrated near the central frequency. Compared with sinc function, Gaussian function

has less sideband. We can use the Gaussian approximation ($\mathrm{sinc}(x) \approx \mathrm{e}^{-\gamma x^2}, \gamma = 0.193$) to replace the sinc function of PMA, then JSA is updated with

$$f(\nu_\mathrm{s}, \nu_\mathrm{i}) = \mathrm{e}^{-\frac{1}{2}(\frac{\nu_\mathrm{s}+\nu_\mathrm{i}}{\sigma_\mathrm{p}})^2} \mathrm{e}^{-\frac{\gamma L^2 \Delta k^2}{4}}, \tag{14}$$

which can be expanded as

$$\begin{aligned} & f(\nu_\mathrm{s}, \nu_\mathrm{i}) \\ = & \exp\left(-\left[\frac{1}{2\sigma_\mathrm{p}^2} + \frac{\gamma L^2}{4}(k'_\mathrm{p} - k'_\mathrm{s})^2\right] {\nu_\mathrm{s}}^2\right) \\ & \times \exp\left(-\left[\frac{1}{2\sigma_\mathrm{p}^2} + \frac{\gamma L^2}{4}(k'_\mathrm{p} - k'_\mathrm{i})^2\right] {\nu_\mathrm{i}}^2\right) \\ & \times \exp\left(-\left[\frac{1}{\sigma_\mathrm{p}^2} + \frac{\gamma L^2}{2}(k'_\mathrm{p} - k'_\mathrm{s})(k'_\mathrm{p} - k'_\mathrm{i})\right] \nu_\mathrm{s}\nu_\mathrm{i}\right). \end{aligned} \tag{15}$$

For Eq. (15), to acquire the spectrally uncorrelated state, the last item of the equation should be eliminated, thus we have

$$\frac{1}{\sigma_\mathrm{p}^2} + \frac{\gamma L^2}{2}(k'_\mathrm{p} - k'_\mathrm{s})(k'_\mathrm{p} - k'_\mathrm{i}) = 0. \tag{16}$$

Given determinate wavelengths of pump, signal, and idler, we can select the suitable pump bandwidth and crystal length to make Eq. (16) hold. As a result, the spectrally uncorrelated state can be achieved.

This is the first method on how to improve the photon purity. It is easy to understand, and can also help us to learn other methods. Moreover, as long as Eq. (16) holds, it should satisfy

$$(k'_\mathrm{p} - k'_\mathrm{s})(k'_\mathrm{p} - k'_\mathrm{i}) < 0. \tag{17}$$

That is to say, the group velocity of the pump should lie between the group velocities of the signal and the idler.

Graphically, the width of PEA's contour is in proportion to the pump bandwidth, and the angle between the contour line and the X axis is 135° due to the law of energy conservation.[15] Here the width of PMA's contour is inversely proportional to the length of the crystal. And its pinch θ is not a fixed value and can be calculated. The tangent for the pinch of PMA can be defined as

$$\tan\theta = -\frac{k'_\mathrm{s} - k'_\mathrm{p}}{k'_\mathrm{i} - k'_\mathrm{p}}. \tag{18}$$

When Eq. (17) holds, the pinch of PMA will be positive.

2.2. Engineering with the group velocity matching condition

We now discuss the second method, to engineer with the GVM conditions.[25–27] GVM conditions can be applied on the pump pulse and at least one daughter photon. The photon pairs are generated in the spectral mode, where the velocity of the pump photon is equal to the group velocity of one daughter photon or the average group velocity of both daughter photons.[5] As a result, spectrally uncorrelated biphoton state and pure heralded single photon are directly generated at several fixed wavelengths. There are three types of GVM conditions[18]

$$V_\mathrm{g,p}^{-1} = V_\mathrm{g,s}^{-1}, \tag{19}$$

$$V_\mathrm{g,p}^{-1} = V_\mathrm{g,i}^{-1}, \tag{20}$$

$$2V_\mathrm{g,p}^{-1} = V_\mathrm{g,s}^{-1} + V_\mathrm{g,i}^{-1}. \tag{21}$$

Equations (19)–(21) are symbolically represented by GVM_1, GVM_2, and GVM_3, respectively. And they are individually consistent with

$$k'_\mathrm{p} = k'_\mathrm{s}, \tag{22}$$

$$k'_\mathrm{p} = k'_\mathrm{i}, \tag{23}$$

$$2k'_\mathrm{p} = k'_\mathrm{s} + k'_\mathrm{i}. \tag{24}$$

As described in Eq. (13), Δk can also be written as

$$\Delta k(\nu_\mathrm{s}, \nu_\mathrm{i}) = (k'_\mathrm{s} - k'_\mathrm{p})\nu_\mathrm{s} + (k'_\mathrm{i} - k'_\mathrm{p})\nu_\mathrm{i}. \tag{25}$$

For GVM_1 or GVM_2, the pump propagates with the same group velocity as one of the daughter photons. Meanwhile, only one daughter photon has an influence on the difference between those wave-vectors, as indicated in Eq. (25). This situation makes PMA (either sinc function or Gaussian function) be extraordinarily asymmetrical for signal and idler. Moreover, the pinch of PMA's contour is 0° or 90°. For GVM_3, if $\nu_\mathrm{s} = \nu_\mathrm{i}$, the influence on the difference between wave-vectors of the signal and the idler will be the same. Meanwhile, the pinch of PMA's contour is 45°, i.e., PMA is perpendicular to PEA. For simplicity, here PMA is assumed as a Gaussian function. The width of its contour is $\frac{\sqrt{2}}{\sqrt{\gamma}L|k'_\mathrm{p} - k'_\mathrm{s}|}$.

As discussed in the previous subsection, in order to reach a high purity, the system parameters should be chosen to make Eq. (16) hold. Moreover, as long as the group velocities of the pump, the signal and the idler satisfy GVM_1 or GVM_2, the pump bandwidth or crystal length tend to be infinite, therefore, Eq. (16) can be rewritten as

$$\frac{\sqrt{2}}{\sigma_\mathrm{p}\tau_\mathrm{s}} + \frac{\sigma_\mathrm{p}\tau_\mathrm{i}}{\sqrt{2}} = 0, \tag{26}$$

where $\tau_\mu = L(k'_\mathrm{p} - k'_\mu)$, $\mu \in \{\mathrm{s}, \mathrm{i}\}$. Physically, τ_μ denotes the delayed value of μ photon with respect to the pump. For GVM_2, $\tau_\mathrm{i} = 0$. Meanwhile, $\tau_\mathrm{s} \gg 1/\sigma_\mathrm{p}$, then the first item of Eq. (26) tends to be zero. Since τ_μ is proportional to the crystal length, a long crystal can be used for achieving spectral uncorrelation. In addition, the pump bandwidth is independent of uncorrelation. And as shown in Ref. [10], varying the pump bandwidth merely alters the ratio of signal width to idler width without affecting the spectral correlation in long crystals. The situation of GVM_1 is similar to that of GVM_2.

For GVM_3, the temporal delays of the signal and the idler are symmetric, indicating that their absolute values are identical but the directions are opposite, i.e., $\tau_s = -\tau_i$. Besides, when $v_s = v_i$, GVM_3 will make the phase-matching condition be satisfied in the entire frequency range of SPDC, and the effects on the phases of parametric lights approximately equal. Therefore, the width of PEA σ_p should be equal to that of PMA $\frac{\sqrt{2}}{\sqrt{\gamma}L|k'_p - k'_s|}$, as indicated in Eq. (16) with GVM_3 holding. As a result, the contour of JSA has a circular shape and two down-converted photons are less correlated. This symmetry source might be good candidates for photon interfering or generating entangled multi-photon sources.

2.3. Uncorrelation by adjusting the width ratio

The methods discussed above adopt the approximation that sinc function is replaced with Gaussian function. However, the approximation could result in deviation between theory and experiment. As discussed in Subsection 2.1, only when PMA is approximated as a Gaussian function,[28] the JSA is factorable and the purity can approach 1. While, the standard shape of PMA is a sinc function, whose the side lobes can destroy the symmetry of the JSA profile. To solve this problem, one can adjust the width ratio between PMA and PEA to improve the photon purity. Firstly, suppose GVM_3 is satisfied and sinc PMA possessing the same width as Gaussian PMA, i.e., $\frac{\sqrt{2}}{L\sqrt{\gamma}|k'_p - k'_s|}$, ξ is defined as the ratio between the widths of PMA and PEA[21]

$$\xi = \frac{\frac{\sqrt{2}}{L\sqrt{\gamma}|k'_p - k'_s|}}{\sigma_p}. \tag{27}$$

Denote

$$\kappa = L(k'_p - k'_s). \tag{28}$$

Then Eq. (27) can be simplified as

$$\xi = \frac{\sqrt{2}}{\sqrt{\gamma}\kappa\sigma_p}, \tag{29}$$

As addressed in Ref. [28], the formula of JSA can be decomposable only when doing approximation on PMA with Gaussian function, and the purity reaches its maximum value when $\xi = 1$. However, without Gaussian approximation, the purity may not be optimal when $\xi = 1$.

Below let us present an improved method on increasing the photon purity. Considering that the expression of ξ in Eq. (27) is asymmetric for the signal and the idler, we re-define an intermediate variable ζ,

$$\zeta = \frac{\frac{\sqrt{2}}{L\sqrt{\gamma}} \frac{1}{\sqrt{-(k'_p - k'_s)(k'_p - k'_i)}}}{\sigma_p}, \tag{30}$$

then the optimal value of ζ can be searched to maximize the purity. Given certain phase-matching central wavelengths, denote $a_1 = k'_p - k'_s$, $a_2 = k'_p - k'_i$, ζ can be simplified as

$$\zeta = \frac{\frac{1}{L}\sqrt{\frac{2}{-\gamma a_1 a_2}}}{\sigma_p}. \tag{31}$$

Obviously, here ζ is only related with the pump wavelength σ_p and the crystal length L. Then the optimal experimental conditions can be found to get the maximum purity.

2.4. Joint optimization of both the pump wavelength and the crystal length

The fourth method is to directly implement joint optimizations on the pump bandwidth and the crystal length in order to obtain the highest purity value within certain spectral ranges. Here we propose to implement the local search algorithm (LSA) into the joint optimization process to replace the trivial exhaustive search method, which can simplify a k-dimensional optimization problem into k one-dimensional optimization problems, greatly reducing the time to search for the optimal values. Though the purity is not able to reach 1 even after applying this method, a proper interference filter can be employed to narrow the bandwidth and further improve the purity.

3. Simulation

Second-order nonlinear optical materials are excellent platforms for quantum optics. For example, potassium titanylphosphate (KTP) and lithium niobate (LN) not only have excellent second-order/third-order nonlinear coefficient and electro-optic effect, but also possess very mature technology on waveguide fabrication. These merits make them very promising candidates for applications in parametric down-conversion, frequency conversion, modulation processes, etc. Here for simplicity, we take periodically poled $KTiOPO_4$ (PPKTP) and periodically poled lithium niobate (PPLN) crystals as examples for descriptions. Their refractive index and Sellmeier equations are referring from Refs. [30,31].

For the first method addressed in Section 2, in order to satisfy the condition (17), we consider the case of type-I non-degenerate PDC. Moreover, for practical application requirements, one of the daughter photons is assumed being located in the communication band (1.3 μm–1.55 μm), then the range of the pump wavelength should lie within 546 nm–632 nm for PPLN and in the range of 756 nm–797 nm for PPKTP. For easy description, we first choose PPKTP as an example, the central wavelengths are chosen as 552 nm, 857.3 nm, and 1550 nm, for the pump, the signal, and the idler photons, respectively. Then the period of the periodically poled is calculated as $\Lambda = 11.6604$ μm, $k'_s - k'_p = 5.782 \times 10^{-12}$ s/m,

and $k'_{\rm i} - k'_{\rm p} = -1.507 \times 10^{-10}$ s/m. To satisfy Eq. (16), $\sigma_{\rm p} L = 1.0906 \times 10^{11}$ Hz·m. If the pump bandwidth $\Delta\lambda$ and the crystal length L are set as 1.5915 nm and 1.1077 cm, respectively, the purity will be 0.99967 when applying Gaussian PMA, while the purity will be 0.96931 when implementing sinc PMA. Accordingly, we plot out corresponding PMA, PEA, and JSA in Fig. 1. Besides, we choose another example of PPLN, the central wavelengths of the pump, the signal, and the idler are set as 775 nm, 1320 nm, and 1877 nm, respectively. Here, $\Lambda = 20.4014$ μm, $k'_{\rm s} - k'_{\rm p} = 2.014 \times 10^{-11}$ s/m, and $k'_{\rm i} - k'_{\rm p} = -2.488 \times 10^{-11}$ s/m. Accordingly, we obtain $\sigma_{\rm p} L = 1.4379 \times 10^{11}$ Hz·m. When the pump bandwidth $\Delta\lambda$ and the crystal length L are 3.1831 nm and 1.4394 cm, respectively, the purity is 0.99877 with Gaussian PMA and 0.94746 with sinc PMA. Corresponding PMA, PEA, and JSA are shown in Fig. 2.

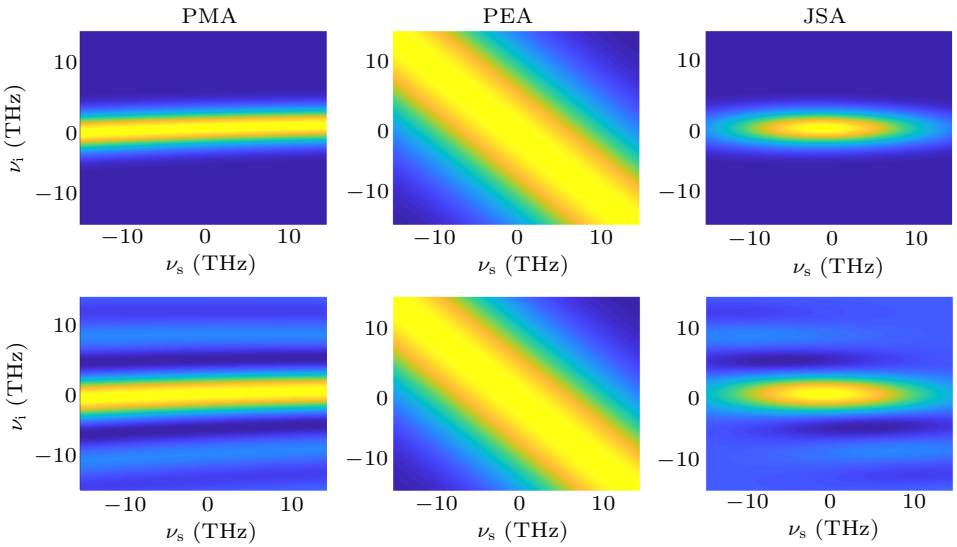


Fig. 1. The contours of PMA, PEA, and JSA in PPKTP simulating with the first method. The biphoton is generated from type-I 552 nm(o)→857.3 nm(e)+1550 nm(e), when the bandwidth $\Delta\lambda$ and the crystal length L are 1.5915 nm and 1.1077 cm, respectively. When PMA is approximated as Gaussian function, PMA, PEA, and JSA are shown in the first row, and the purity is 0.99967. When PMA is adopted with sinc function, PMA, PEA, and JSA are shown in the second row, and the purity is 0.96931.

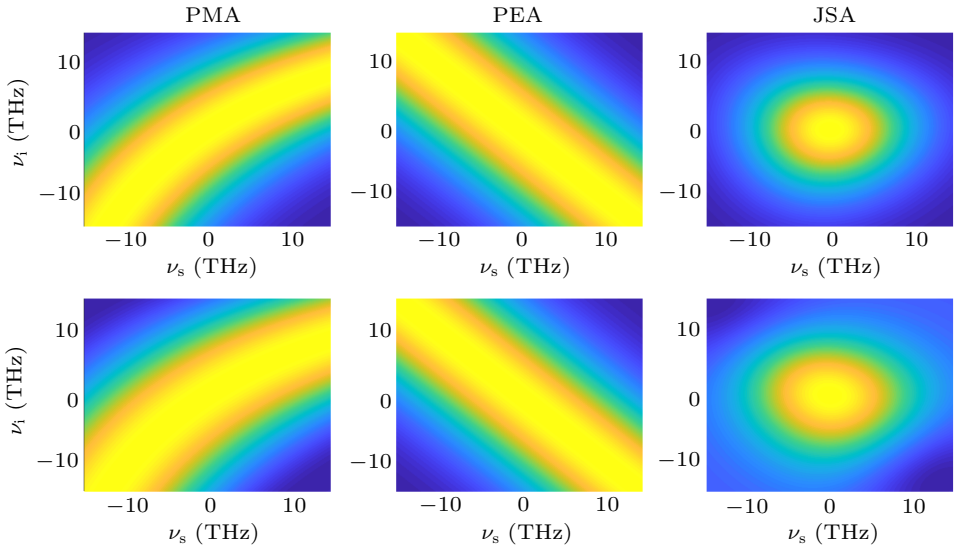


Fig. 2. The contours of PMA, PEA, and JSA in PPLN simulating with the first method. The biphoton is generated from type-I 775 nm(e)→1320 nm(o)+1877 nm(o), when the bandwidth $\Delta\lambda$, the crystal length L, and temperature are 3.1831 nm, 1.4394 cm, and 30 °C, respectively. When PMA is approximated as Gaussian function, PMA, PEA, and JSA are shown in the first row, and the corresponding purity is 0.99877. When PMA is adopted with sinc function, PMA, PEA, and JSA are shown in the second row, and accordingly, the purity is 0.94746.

For the second method, we consider type-II degenerate SPDC. We find that $\rm GVM_1$ is satisfied when the pump wavelength is 612 nm and $\rm GVM_3$ is satisfied when the pump wavelength is 791 nm in PPKTP crystal. For $\rm GVM_1$ or $\rm GVM_2$, a long crystal can be employed to improve the purity. When the pump wavelength is 612 nm, the pump bandwidth and crystal length might be chosen as 2 nm and 3 cm, respectively, accordingly, the purity is 0.98463 and its JSA is shown in Fig. 3(a). For $\rm GVM_3$, the pump bandwidth and crystal length can be selected by following Eq. (16). With the pump wavelength of

791 nm, the pump bandwidth and crystal length can take the values of 0.51 nm and 1 cm, respectively. Then the purity is 0.81429 and its JSA is shown in Fig. 3(b).

Now, let us see the third method presented in Section 2, where GVM_3 is assumed to be satisfied. We analyze the relationship between ξ defined in Eq. (27) and purity for two different types of PMAs, as illustrated in Fig. 4(a). It shows that the maximum purity can reach 1 when $\xi = 1$ for Gaussian shaped PMA. However, for sinc shaped PMA, the purity just reaches its maximum value when $\xi = 1.14$ and its maximum purity is 0.8146. Obviously, it only results in poor purity. Now let us see our improved method, the relationships between ζ defined in Eq. (30) and purity are displayed out for two different types of PMAs, see Fig. 4(b). For easy description, here we use type-I 775 nm→ 1320 nm+1877 nm in PPLN as an example. As we can see from Fig. 4(b), the purity reaches its maximum for the sinc shaped PMA when $\zeta = 1.21$, and its maximum value is 0.97924, where the pump bandwidth $\Delta\lambda$ and the crystal length L are 3.1831 nm and 1.1896 cm, respectively. Compared with the above maximum purity 0.8146, our modified method shows significant improved purity.

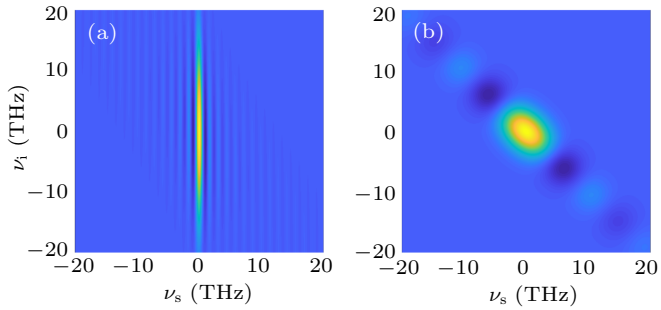


Fig. 3. The contours of JSA for different wavelength matchings simulating with the second method. (a) The biphoton is generated from type-II 612 nm(o)→ 1224 nm(e)+1224 nm(o) in PPKTP and the purity is 0.98463, when the bandwidth $\Delta\lambda$ and the crystal length L are 2 nm and 3 cm. (b) The biphoton is generated from type-II 791 nm(o)→ 1582 nm(e)+1582 nm(o) in PPKTP and the purity is 0.81429, when the bandwidth $\Delta\lambda$ and the crystal length L are 0.51 nm and 1 cm.

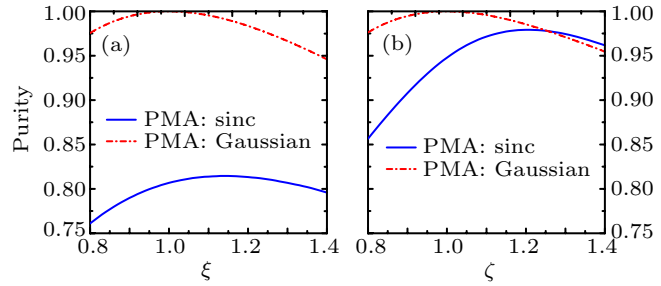


Fig. 4. (a) The relationship between ξ and purity for Gaussian PMA and sinc PMA with GVM_3. (b) The relationship between ζ and purity for Gaussian PMA and sinc PMA for type-I 775 nm→ 1320 nm+1877 nm in PPLN with the improved third method.

For the fourth method, considering it does not need to satisfy any limitations on either inequality (17) or GVM conditions, it is a more general approach and has robust applications. For easy description, we use type-I PPKTP as an example, where the central wavelengths of pump, signal, and idler are set as 552 nm, 857.3 nm, and 1550 nm, respectively. We carry out jointly optimizing on both the pump band width and the crystal length, corresponding simulation results are shown in Fig. 5. From Fig. 5, we find that the purity can reach up to 1 after full parameter optimizations. If taking practical processing difficulty into account, we can select compromised pump bandwidth $\Delta\lambda$ and crystal length L, e.g., 2 nm and 8.8 mm, respectively, and the corresponding purity is 0.94569. Obviously, the fourth method is not only easy to implement, but also can show excellent performance.

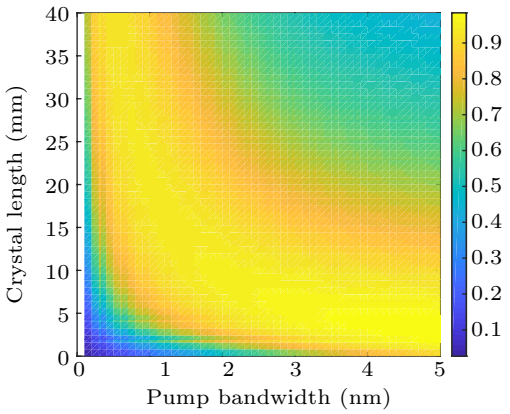


Fig. 5. Joint optimization of the pump bandwidth and crystal length with the fourth method. Meanwhile, the central wavelengths of pump, signal, and idler are 552 nm, 857.3 nm, and 1550 nm, respectively in type-I PPKTP. Different color represents different purity, and the value of purity represented by the color has been marked on the right column.

In addition, we also carried out calculations for other nonlinear crystals or phase-matching conditions, e.g., type-II BBO or type-0 PPLN, by implementing the above four methods. However, the obtained purities are in general quite low when without using filters. Therefore, we did not list them out in the simulation part.

4. Conclusion

Focusing on collinear and single mode SPDC and neglecting transversal and multi-mode effects, we have discussed four methods on how to improve the purity of down-converted photon sources. The first method is to derive from JSA function, through which we can obtain the relationship between the pump bandwidth and the crystal length for spectral uncorrelation. The second method is taking advantage of GVM conditions. The third method is to adjust the width ration of PEA and PMA under GVM_3 condition, without doing any approximation on PMA functions. The fourth method is to apply joint optimization on both the pump bandwidth and the crystal length without doing any approximation or assuming any GVM condition. For the first three methods, they need to meet certain applicable conditions, e.g., it needs to satisfy the inequality for method 1 or method 3; and the second method only works when satisfying one of the GVM conditions. For

the fourth method, it does not assume any applicable conditions, while for some phase-matching conditions, sometimes resulting in moderate purities without filters. Therefore, different methods have their advantages and disadvantages, and a proper method should be chosen when people design their experimental parameters. We believe our work could provide valuable references for the generation and application of high purity single-photon sources in the fields of quantum information and quantum optics.

References

[1] Zhang C H, Zhang C M, Guo G C and Wang Q 2018 *Opt. Express* **26** 4219
[2] Zhang C H, Zhang C M and Wang Q 2019 *Phys. Rev. A* **99** 052325
[3] Sang M L, Lee S W, Jeong H and Park H S 2020 *Phys. Rev. Lett.* **124** 060501
[4] Mattle K, Weinfuter H, Kwiat P G and Zeilinger A 2002 *Rev. Mod. Phys.* **74** 145
[5] Mosley P J, Lundeen J S, Smith B J, Wasylczyk P, U'Ren A B, Silberhorn C and Walmsley I A 2008 *Phys. Rev. Lett.* **100** 133601
[6] Meyer-Scott E, Montaut N, Tiedau J, Sansoni L, Herrmann H, Bartley T J and Silberhorn C 2017 *Phys. Rev. A* **95** 061803
[7] Brańczyk A M, Ralph T C, Helwig W and Silberhorn C 2010 *New J. Phys.* **12** 063001
[8] Christ A, Lupo C, Reichelt M, Meier T and Silberhorn C 2014 *Phys. Rev. A* **90** 023823
[9] Chen C, Cao B, Niu M Y, Xu F, Zhang Z, Shapiro J H and Wong F N C 2017 *Opt. Express* **25** 7300
[10] U'Ren A B, Silberhorn C, Erdmann R, Banaszek K, Grice W P, Walmsley I A and Raymer M G 2005 *Laser Phys.* **15** 146
[11] Mosley P J, Lundeen J S, Smith B J and Walmsley I A 2008 *New J. Phys.* **10** 093011
[12] Bruno N, Martin A, Guerreiro T, Sanguinetti B and Thew R T 2014 *Opt. Express* **22** 17246
[13] Zhang Q Y, Xue G T, Xu P, Gong Y X, Xie Z and Zhu S 2018 *Phys. Rev. A* **97** 022327
[14] Kaneda F, Palmett K G, U'Ren A B and Kwiat P G 2016 *Opt. Express* **24** 10733
[15] Jin R B, Shimizu R, Wakui K, Benichi H and Sasaki M 2013 *Opt. Express* **21** 10659
[16] Jin R B, Shimizu R, Wakui K, Fujiwara M, Yamashita T, Miki S, Terai S, Wang Z and Sasaki M 2014 *Opt. Express* **22** 11498
[17] Jin R B, Gerrits T, Fujiwara M, Wakabayashi R, Yamashita T, Miki S, Terai H, Shimizu R, Takeoka M and M. Sasaki 2015 *Opt. Express* **23** 28836
[18] Jin R B, Cai N, Huang Y, Hao X Y, Wang S, Li F, Song H Z, Zhou Q and Shimizu R 2019 *Phys. Rev. Appl.* **11** 034067
[19] Weston M M, Chrzanowski H M, Wollmann S, Boston A, Ho J, Shalm L K, Verma V B, Allman M S, Nam S W, Patel R B, Slussarenko S and Pryde G J 2016 *Opt. Express* **24** 10869
[20] Giovannetti V, Maccone L, Shapiro J H and Wong F N C 2002 *Phys. Rev. Lett.* **88** 183602
[21] Graffitti F, Kelly-Massicotte J, Fedrizzi A and Brańczyk A M 2018 *Phys. Rev. A* **98** 053811
[22] Laudenbach F, Jin R B, Greganti C, Hentschel M, Walther P and Hübel 2017 *Phys. Rev. Appl.* **8** 024035
[23] Grobe R, Rzazewski K and Eberly J H 1994 *J. Phys. B: At. Mol. Phys.* **27** L503
[24] Yu T and Eberly J H 2004 *Phys. Rev. Lett.* **93** 140404
[25] Keller T E and Rubin M H 1997 *Phys. Rev. A* **56** 1534
[26] Grice W P, U'Ren A B and Walmsley I A 2001 *Phys. Rev. A* **64** 063815
[27] Edamatsu K, Shimizu R, Ueno W, Jin R B, Kaneda F, Yabuno M, Suzuki H, Nagano S, Syouji A and Suizu K 2011 *Prog. Inform.* **8** 19
[28] Quesada N and Brańczyk A M 2018 *Phys. Rev. A* **98** 043813
[29] Zhou X Y, Zhang C M and Wang Q 2017 *Journal of the Optical Society of America B* **34** 1518
[30] Dmitriev V G, Gurzadyan G G and Nikogosyan D N 1999 *Handbook of Nonlinear Optical Crystals* 3rd edn. (Springer-Verlag Berlin Heidelberg)
[31] Gayer O, Sacks Z, Galun E and Arie A 2008 *Appl. Phys. B* **91** 343